



Published in final edited form as:

Technology (Singap World Sci). 2015 June ; 3(4): 172–178. doi:10.1142/S2339547815200058.

Quantitative assessments of glycolysis from single cells

Young Shik Shin^{1,3,*}, Jungwoo Kim^{3,*}, Dazy Johnson¹, Alex A. Dooraghi², Wilson X. Mai¹, Lisa Ta¹, Arion F. Chatziioannou², Michael E. Phelps^{1,2,3}, David A. Nathanson¹, and James R. Heath^{1,3}

¹Department of Molecular and Medical Pharmacology, David Geffen School of Medicine, University of California, Los Angeles, CA 90095, USA

²Crump Institute for Molecular Imaging, University of California, Los Angeles, CA 90095, USA

³NanoSystems Biology Cancer Center, Division of Chemistry and Chemical Engineering, California Institute of Technology, Pasadena, CA 91125, USA

Abstract

The most common positron emission tomography (PET) radio-labeled probe for molecular diagnostics in patient care and research is the glucose analog, 2-deoxy-2-[F-18]fluoro-D-glucose (¹⁸F-FDG). We report on an integrated microfluidics-chip/beta particle imaging system for *in vitro* ¹⁸F-FDG radioassays of gl

INNOVATION

Recent advances in single cell proteomics, genomics, and transcriptomics methods have shown promise towards uncovering fundamental biological phenomena that are unresolved when bulk cell populations are interrogated^{1,2}. By contrast, single cell metabolic assays have remained relatively unexplored, although recent progress in both mass spectrometric³ and microchip methods is promising⁴. The rapid response of cellular metabolic responses to many drugs makes metabolic assays a valuable tool for rapid screening assays and investigating early biological responses to treatments. Such assays, if carried out at the single cell level, have the potential to identify metabolic outliers — i.e. individual cells exhibiting responses to drugs that are well above or below the population average. The identification of such outliers in a manner that permits further analysis at the genomic or transcriptomic level may offer new insights for understanding therapeutic resistance. We report on an integrated microfluidic chip/beta-particle imaging camera (the Betabox) that is a first step for enabling such questions to be explored.

Correspondence should be addressed to J.R.H. (heath@caltech.edu) and Y.S.S. (ysshin@mednet.ucla.edu)..

*These authors contributed equally to this work.

AUTHOR CONTRIBUTIONS

Y.S.S. and J.K. developed microfluidic device, designed and performed tests. D.J., W.X.M., and L.T. prepared biological samples for tests. A.A.D. and A.F.C. developed the Betabox camera and software. D.A.N. and M.E.P. provided detailed guidelines and discussion for the experimental design and interpretation of the results. Y.S.S., J.K., and J.R.H. wrote the manuscript. J.R.H. and Y.S.S. directed the research.

COMPETING INTERESTS STATEMENT

M.E.P., A.F.C., and J.R.H. are founders and stockholders in Sofie Bio-sciences, Inc., which is seeking to commercialize certain aspects of the Betabox technology.

NARRATIVE

An accelerated rate of aerobic glycolysis within many tumors (the Warburg effect) provides the diagnostic basis for using ^{18}F -FDG as a PET *in vivo* molecular imaging probe⁵ of the rate of glycolysis within tumors. ^{18}F -FDG PET can also be used to image the metabolic responses of those tumors to drugs. In a similar manner, ^{18}F -FDG can serve as a radio-labeled probe to measure altered states of glycolysis in cancer cells *in vitro*, including alterations in glycolytic rates that are induced by therapeutic interventions. We recently reported on a microfluidic platform mated to a beta particle imaging camera of the Betabox⁶⁻⁸. The Betabox was used to analyze the short time frame (~hour) influence of targeted inhibitors on glycolysis in cell populations. We measured the glycolytic response of the model glioblastoma (GBM) cell line, U87EGFRvIII, to inhibition of the epidermal growth factor receptor (EGFR) by erlotinib⁶. As anticipated from PET ^{18}F -FDG in cancer patients, erlotinib treatment of the U87E-GFRvIII cells reduced the rate of glycolysis, although, surprisingly, that reduction was uneven over the 4 hours following start of treatment. This uneven decrease in glycolysis was accompanied by oscillations in the levels of various phosphoproteins downstream of EGFR signaling.

In the present study, we report on a redesign of the Betabox that permits a similar kinetic study, but at the level of single cells. The modified Betabox is shown to be sufficiently sensitive and quantitative that the variance of glycolysis across a statistical number of single cells is resolved for the first time. The assay is non-destructive to the cells, and the results may be integrated with optical microscopy measurements that permit the rates of glycolysis to be compared against cell size.

The Betabox is composed of two chips; a position-sensitive silicon avalanche photodiode detector to image and measure beta-particle emission from probes radio-labeled with positron emitting isotopes, ^{14}C , ^{18}F , etc., and a polydimethylsiloxane (PDMS) microfluidic chip for capturing cells in culture media. The microfluidic chip is placed on the Si camera. The layout of the Betabox with representative examples of microfluidic chip designs containing cell traps is illustrated in **Fig. 1**. The Si camera can image and measure beta particle emission simultaneously from each of the cell traps. The Si camera of the Betabox has been previously validated and described elsewhere^{7,8}.

The microfluidic chip is a 2-layer device fabricated with standard photolithography and rapid prototyping methods (see **Supplementary Information**)⁹. The chips used for this study have either 4 or 5 cell capture microchambers in each of 5 or 6 separate channels, respectively. Thus, each microfluidic chip has either 20 or 30 chambers as an array format of 4 by 5 or 5 by 6. All the chambers can be used for a single test condition by sharing a common inlet (**Fig. 1b**). A modified design with separate inlets and outlets for each channel permits 5 or 6 independent assays per chip, such as those required to perform a kinetic study (**Supplementary Fig. 1d** in the **Supplementary Information**). Several features in the chip design promote high signal sensitivity and single cell spatial resolution. The first feature is a thin bottom membrane of the chip that separates the cells from the camera, and is designed to minimize signal attenuation of the beta particles emitted by radio-labeled probe in the microfluidic chip. We tested several membrane thicknesses by utilizing various spin coating

speeds during the PDMS bottom layer fabrication step (**Supplementary Fig. 2**). A 13 μm -thick membrane was found to offer an optimized combination of signal sensitivity and mechanical strength, and yielded 20% increase in the sensitivity for detecting the beta particle emission from the radio-labeled probes relative to our previous design (**Supplementary Fig. 2**)⁶. A second design feature is the cell traps that are drawn from previous literature^{10,11}. The cell traps, coupled with the transparent microfluidic chip, permit direct observation and recording of which traps contain single cells. The optical image can be registered with the Si camera image to assign rates of glycolysis to the individual cells. A third feature is the inlet filters, that are designed to prevent particles and clumped cells from clogging the active areas of the microfluidic chip. Design details are shown in **Supplementary Fig. 1**.

The Betabox performance was evaluated by using phantoms that were printed using an inkjet on glossy photographic paper. The printed pattern replicated the microfluidic chip design, with each location containing ^{18}F -FDG (**Fig. 1b,2a**)^{7,12}. The Si camera recording of beta particle emission from each location of the phantom showed a 5% of coefficient of variation (CV) (**Supplementary Table 2**). This variation is likely attributable to small variations in the PDMS membrane thickness, but, whatever the source is, the low CV value indicates that the intrinsic error of the Betabox is low. A related, previously reported evaluation that was designed to account for the inkjet printer error revealed a CV of below 2%⁷. A time course measurement of the ^{18}F decay curve from the phantom was also recorded over a 12-hour period at 15-minute intervals (**Fig. 2b**). The measured time-dependence of the activities follows the known ^{18}F half-life of 109.8 minutes. This result provides calibration data for combining results from multiple independent Betabox measurements, thus significantly increasing the statistical sampling of the single cell measurements.

The Betabox design, with its 5 independent microchannels, each designed with a selected number of cell traps, permits kinetic assays of glycolysis under drug treatments at the single cell level (**Supplementary Fig. 1d**). As a demonstration, we measured the alteration in glycolysis of a patient-derived, EGFR over-expressing glioblastoma neurosphere tumor model (GBM39) to EGFR inhibition with erlotinib¹³. We determined glycolysis at 1, 4, 12, and 24 hours following start of treatment versus the untreated control (**Fig. 3a–d**). To validate the single cell platform, 2 experimental assays were compared. The first was a Betabox design with 5 independent channels, each containing 4 chambers with 40-cell traps (**Supplementary Fig. 1d**). The ~40–50% reduction in glycolysis following 24 hours erlotinib treatment (**Fig. 3a,b**) is in reasonable agreement with both *in vivo* measurements (using ^{18}F -FDG PET) of a GBM39 mouse xenograft tumor model⁴. The Betabox platform, applied to cell populations, has also been previously validated against bulk *in vitro* radioassays using standard methods⁶. These results indicate that the 40-cell trap design (**Fig. 1c**) yields a reliable population-based analysis.

The second assay was with a Betabox designed for single cell resolution: 5 microchannels, each containing 4 chambers with a single cell trap (**Fig. 1c,bottom**). GBM39 cells have been shown previously to exhibit decreased glycolysis with ^{18}F -FDG upon erlotinib treatment¹³. The 40-trap device captured a slightly increased signal with 1-hour treatment, followed by a

significant decrease at 12 and 24 hours (**Fig. 3b**). Averaged signal intensities of single cells showed a similar response, although the single cell measurements provided additional information that demonstrated the heterogeneity of glycolytic alterations within individual cells (**Fig. 3d**). For a more in-depth analysis of the heterogeneity, we chose two conditions (control vs. 24 hours erlotinib treatment) and tested them with a set of five microfluidic chips per condition. These independent measurements were corrected for the decay of ^{18}F activity based on the calibration data and then, for each separate condition, combined. Out of 100 cell traps, 43 and 46 traps captured single cells for the control and the drug-treated condition, respectively. Erlotinib treatment decreased glycolysis by approximately 40%, with a standard deviation that was decreased by ~55%, relative to control. This measured variance in glycolysis of GBM39 cells is an important aspect of the Betabox technology as the metabolic outliers may have value for understanding therapeutic resistance¹⁴.

The transparency of the PDMS microfluidic chip, coupled with knowledge of the cell-trap locations, permits simultaneous measurements of cell morphology and size. GBM39 cells, by their nature, are characterized by a broad distribution of cell sizes. In these Betabox studies, it is straightforward to determine whether the heterogeneity in cell size is associated with a corresponding heterogeneity in glycolysis. We investigated this relationship for 58 single cells. Images of cells for the two extreme cases are shown in **Fig. 4a**. Even though the two extreme cases point to a correlation between cell size and glycolysis, only a weak positive correlation (Spearman correlation of 0.36 with p -value of 0.006) was detected when the whole population was analyzed (**Fig. 4b**). Using a single cell barcode chip (SCBC) platform, we recently reported on a combined analysis of metabolites and phosphoprotein signaling pathways from statistical numbers of single cells separated from a GBM39 tumor model. In that study, we found two metabolic phenotypes dominate the measured cellular heterogeneity: 80% of the cells exhibit high glucose uptake and low cAMP and cGMP, while 20% of the cells exhibit high cAMP and cGMP, but low glucose uptake⁴. Unlike the betabox, the SCBC analysis is destructive to the cells, and so the gene regulatory networks that underlie this metabolic heterogeneity could not be identified. However, the single cell Betabox platform should permit the metabolic outliers to be further analyzed via exome or transcriptomic analysis. This is a major power of the Betabox platform.

We have demonstrated a Betabox design that has sufficient sensitivity and spatial resolution to provide images and robust/quantitative measurements of glycolysis with ^{18}F -FDG in single cells. We applied this technology for quantitative assays of glycolysis in single GBM cells over a time period of a few hours following erlotinib treatment. The variance in glycolysis across a statistical number of single cells was resolved. For both control and drug treated cells, the variation in glycolysis across single cells was broad, with standard deviation values of approximately 92% and 66% of the average, respectively. Furthermore, this variation exhibited only a weak correlation with the broad distribution of cell sizes that is characteristic of the GBM39 cells. The Betabox assay is non-destructive to the cells, and so further molecular analysis of the radioassayed cells should permit deeper insights into this heterogeneity¹⁵. In addition, there is a wide range of available PET probes for various metabolic, signal transduction, synthetic processes associated with disease states¹⁶. The Betabox can thus serve as a valuable tool for quantitating the heterogeneity of various

biological functions in single cells and for helping explore the implications of that heterogeneity in disease and disease treatments.

METHODS

Betabox assay platform

The Betabox assay platform consists of a silicon-based β -particle imaging camera (Betabox camera) and a polydimethylsiloxane (PDMS)-based microfluidic chip (Betabox device). The Betabox camera was validated and operated as previously described⁶⁻⁸. The design in this paper is developed based on the general considerations of previous work⁶. The current version of the Betabox device, however, has improved the measurement sensitivity about 20% by implementing a thinner bottom PDMS film (13 μm , instead of 50 μm used in previous report) between position-sensitive avalanche photodiode (PSAPD, Radiation Monitoring Devices) and the cells. This improvement in measurement sensitivity enables single cell-based metabolic measurements. To make the fabrication process simpler, all the features including the dust filter and cell traps are moved to the top layer.

The Betabox microchip device has 3 key features: 1) a cell trap array, 2) inlet filters, and 3) a perfusion channel (**Fig. 1** and **Supplementary Fig. 1**). Different designs permit different numbers of cell traps (1-, 7-, or 40-cell traps) depending on the purpose of the study. Each individual cell trap consists of 2 micro hurdles with 5 μm gap. The shape of the cell trap was optimized to minimize the chance of trapping more than one cell per chamber (**Supplementary Fig. 1c**). We utilized two different configurations of solution inlets. By sharing a single inlet for all the channels, we can test a single condition per device (**Fig. 1b**). Testing multiple conditions, such as in a kinetic study, is enabled by placing independent inlets/outlets for each channel (**Supplementary Fig. 1d**). The inlet filters are essential for preventing dust, cell debris or clumped cells from blocking the active region of cell traps. Detailed shape, layout and dimensions of the filter region are shown in **Supplementary Fig. 1b**. Two sets of inlets and filters are placed upstream to minimize the failure rate of the device due to unexpected clogging.

Analysis on single cells can be achieved by measuring multiple devices for a single condition. As described in the main text (**Fig. 2**), the Betabox signals can be adjusted to a single time point (usually the first or the last time point) based on calibrations against the decay of ¹⁸F-FDG radioactivity. Cell loading efficiency for cell traps is around 90%. However, a single trap can capture two or more cells and trapped single cells can be lost during the handling. The final loading efficiency for single cells is 50–80%. Currently up to 20 Betabox devices can be measured in a single day and the yield of single cell measurement will be improved through the further optimization of the test protocol.

Betabox device fabrication

The Betabox device consists of 2 PDMS layers fabricated by standard soft lithography methods. The top layer is ~5 mm thick, and contains all the described key features of the Betabox device in microchannels with ~30 μm height. The top layer is molded with a master fabricated by standard photolithography with SU-8 2025 photoresist (Microchem) on a

silicon wafer. The master is treated with chlorotrimethylsilane (TMCS, Sigma-aldrich) for 10 minutes before each use; 10 : 1 mixture (w/w) of PDMS prepolymer and curing agent (Sylgard 184@1, Corning) was poured onto the master, degassed in a vacuum chamber, and baked at 80 °C for 2 hours. The cured PDMS slab was peeled off from the master, and holes for inlets and outlets were punched. The bottom layer used in this study is ~13 µm thick, and it does not contain any features. 25 mm × 75 mm sized, 1 mm thick, pre-cleaned glass slides (Gold Seal® Microslides) were cleaned with piranha solution (3 sulfuric acid : 1 hydrogen peroxide, v/v) at 120 °C for 20 minutes followed by thorough rinsing with distilled water and drying at 80 °C for 20 minutes. Dried glass slides were treated with TMCS for 30 minutes. The degassed 10 : 1 mixture (w/w) of PDMS prepolymer and curing agent was poured onto the treated glass slide and was spun at 4000 rpm for 1 minute followed by baking at 80 °C for 1 hour. The top and bottom PDMS layers were irreversibly bonded by plasma treatment (PDC-32G, Harrick Plasma) for 1 minute.

System evaluation with radioactive phantoms

Radioactive phantoms were prepared based on the Betabox device layout by printing a mixture of ink and ¹⁸F-FDG solution on Epson Ultra Premium photo paper GLOSSY with an inkjet printer (Canon iP4700 printer). The ink cartridge was emptied prior to printing the radioactive phantoms; 1 mL of ink mixture containing 3.7×10^7 Bq/mL ¹⁸F-FDG was prepared and injected into the ink cartridge. The level of radioactivity was adjusted with a radiometer (ATOMLAB™ 500 BIO-DEX). β-particles, generated from the disintegration of printed ¹⁸F-FDG pattern, were captured by the Betabox with 5 minutes of acquisition time. The results were used to check the measurement error of the Betabox by location and to calibrate the decay of ¹⁸F-FDG radioactivity (**Fig. 2** and **Supplementary Table 2**).

Cell culture and drug treatment

GBM39 primary neurospheres were cultured in Dulbecco's Modified Eagle Media Nutrient Mix F-12 (DMEM/F12, Invitrogen) supplemented with B27 (Invitrogen), Glutamax (Invitrogen), Heparin (1 µg/mL), Epidermal Growth Factor (EGF, 20 ng/mL, Sigma), Fibroblast Growth Factor (FGF, 20 ng/mL, Sigma) and 100 U/mL of penicillin and streptomycin (Gibco) in a humidified 5% CO₂ (v/v) incubator, at 37 °C. For the drug treatment, 1 million cells were suspended in 10 mL of media containing 1 µM erlotinib (ChemieTek). The cells were then treated for designated periods of time and processed for tests.

The Betabox assay procedures

¹⁸F-FDG treatment—Single cell suspension was prepared from the GBM39 neurospheres or the Erlotinib treated, pre-dissociated cells; 1×10^6 cells/mL were treated with 3.7×10^7 Bq/mL ¹⁸F-FDG in the glucose free medium (**Supplementary Table 1**) in a 5% CO₂ (v/v) humidified incubator at 37 °C for 1 hour. After treatment, cells were washed with the full medium three times to remove residual unbound ¹⁸F-FDG.

Betabox measurement—The device was first filled with glucose free medium before the assay was executed; 5–10 µL of ¹⁸F-FDG treated GBM39 cells, prepared at a concentration of 2×10^6 cells/mL in the glucose free medium, were loaded by applying negative pressure

with a 1 mL syringe from the outlet. After cell trapping, about 80 μ L of glucose free media was flown to remove untrapped cells. For the measurement, the Betabox device was aligned with the Betabox camera and image was acquired for 5 minutes. A custom-coded Matlab (Natick, MA) program was used to control the Betabox, collect and analyze the data. After radioactivity measurement, optical images of the captured cells were recorded with a microscope (Nikon Eclipse Ti-S) for cell count and size measurement.

Data analysis—Depending on the Betabox device design, 20 or 30 rectangular regions of interest (ROIs) were set on the radio-image, and the total measured β -particle count in each ROI was quantified by the custom-coded Matlab program. The average of the total β -particle count from all the empty chambers was used as the background level. This background level was subtracted from the total β -particle count for each chamber with cells. Counts per minute (CPM) refers to the actual total β -particle counts from a chamber divided by the acquisition time (5 minutes for this study). CPM/cell values were calculated, dividing CPM by the number of captured cells in a chamber. CPM/cell data, from multiple Betabox assays in a day, were adjusted considering the time interval between the assays based on the calibration data. Since the detected decay of the ^{18}F -FDG radioactivity exactly follows the theoretical prediction, all the data obtained at different time points could be adjusted to the ones at a single time point for direct comparison. Cell size was measured from the optical image with ImageJ (NIH). Equivalent diameter of each cell was calculated based on the 2D area of captured cells. Cell volume calculated with the equivalent diameter (with the assumption that a cell has a spherical shape) was used for the correlation analysis.

Statistical analysis

The levels of glycolysis were measured as CPM/cell and mean values plus and minus the standard deviation were also presented along with the single cell measurement values. To compare control and erlotinib-treated groups with various treatment times unpaired, two-tailed student *t*-tests were performed to determine whether the conditions produced significantly different results. *p* values less than or equal to 0.05 were considered statistically significant. For the correlation analysis between cells size and glycolysis level, Spearman correlation value was calculated between cell volume and CPM and the correlation value was 0.36 (*p* value = 0.006).

Supplementary Material

Refer to Web version on PubMed Central for supplementary material.

ACKNOWLEDGEMENTS

This work was supported by the National Cancer Institute grant 5U54 CA151819 (JRH PI), the Ben and Catherine Ivy Foundation, the Jean Perkins Foundation, the NCI In Vivo Cellular and Molecular Imaging Center (ICMIC) and the Phelps Family Foundation. A.D. was supported in part by the UCLA Scholars in Oncologic Molecular Imaging program, NIH grant R25T CA098010. Y.S.S. acknowledges the support from the Korean-American Scientists and Engineers Association (KSEA).

REFERENCES

1. Yu J, et al. Microfluidics-based single-cell functional proteomics for fundamental and applied biomedical applications. *Ann. Rev. Anal. Chem.* 2014; 7:275–295.
2. Blainey PC, Quake SR. Dissecting genomic diversity, one cell at a time. *Nat. Methods.* 2014; 11:19–21. [PubMed: 24524132]
3. Zenobi R. Single-cell metabolomics: Analytical and biological perspectives. *Science.* 2013; 342:1243259. [PubMed: 24311695]
4. Xue M, et al. Chemical methods for the simultaneous quantitation of metabolites and proteins from single cells. *J. Am. Chem. Soc.* 2015; 137:4066–4069. [PubMed: 25789560]
5. Gatenby RA, Gillies RJ. Why do cancers have high aerobic glycolysis? *Nat. Rev. Cancer.* 2004; 4:891–899. [PubMed: 15516961]
6. Wang J, et al. Fast metabolic response to drug intervention through analysis on a miniaturized, highly integrated molecular imaging system. *J. Nucl. Med.* 2013; 54:1820–1824. [PubMed: 23978446]
7. Dooraghi AA, et al. Betabox: A beta particle imaging system based on a position sensitive avalanche photodiode. *Phys. Med. Biol.* 2013; 58:3739–3753. [PubMed: 23656911]
8. Vu NT, et al. A beta-camera integrated with a microfluidic chip for radioassays based on real-time imaging of glycolysis in small cell populations. *J. Nuc. Med.* 2011; 52:815–821.
9. Duffy DC, McDonald JC, Schueller OJ, Whitesides GM. Rapid prototyping of microfluidic systems in poly(dimethylsiloxane). *Anal. Chem.* 1998; 70:4974–4984. [PubMed: 21644679]
10. Di Carlo D, Wu LY, Lee LP. Dynamic single cell culture array. *Lab Chip.* 2006; 6:1445–1449. [PubMed: 17066168]
11. Wheeler AR, et al. Microfluidic device for single-cell analysis. *Anal. Chem.* 2003; 75:3581–3586. [PubMed: 14570213]
12. van Staden JA, et al. Production of radioactive quality assurance phantoms using a standard inkjet printer. *Phys. Med. Biol.* 2007; 52:N329–337. [PubMed: 17634634]
13. Nathanson DA, et al. Targeted therapy resistance mediated by dynamic regulation of extrachromosomal mutant EGFR DNA. *Science.* 2014; 343:72–76. [PubMed: 24310612]
14. DeBerardinis RJ, Thompson CB. Cellular metabolism and disease: What do metabolic outliers teach us? *Cell.* 2012; 148:1132–1144. [PubMed: 22424225]
15. Patel AP, et al. Single-cell RNA-seq highlights intratumoral heterogeneity in primary glioblastoma. *Science.* 2014; 344:1396–1401. [PubMed: 24925914]
16. Czernin J, Phelps ME. Positron emission tomography scanning: Current and future applications. *Ann. Rev. Med.* 2002; 53:89–112. [PubMed: 11818465]

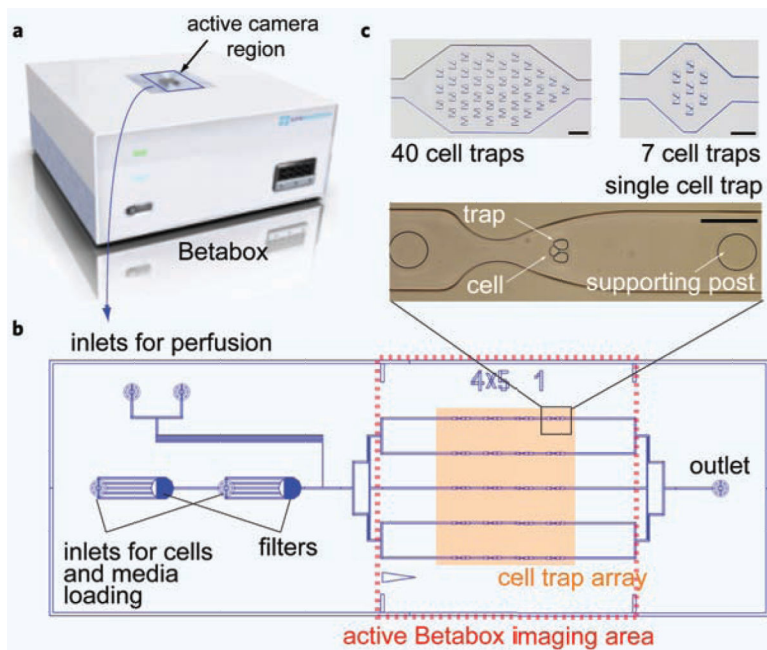


Figure 1. Functional layout of the Betabox. (a) The silicon chip camera and electronics of the Betabox showing the active imaging area. (b) A schematic drawing of the PDMS microfluidic chip, illustrating the region that is viewed by the active area of the Si camera. (c) Optical image of a single cell trap with a captured cell (bottom) and examples of cell trap array designs in which the numbers of trapped single cells can be varied (top). Scale bars: 100 μm .

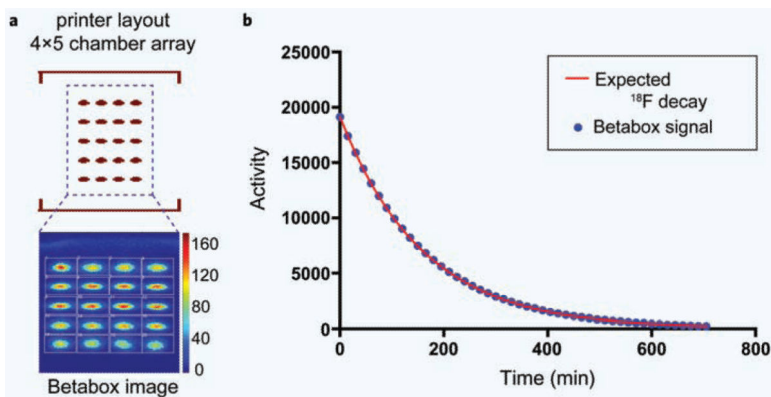


Figure 2.

Betabox evaluation with a phantom that had 20 spots printed with ^{18}F -FDG. (a) Image of the phantom layout used for evaluating the Betabox performance (top) and the actual acquired image of the printed pattern with the Betabox (bottom). The beta particle emission is recorded from each of the 20 locations for 5 minutes by the Si camera to form the image. (b) ^{18}F beta particle emission was recorded over a 12-hour period to determine if the dynamic range of the Betabox would be sufficient to yield the correct half-life of ^{18}F . Activity of each time point is the averaged total counts of all 20 locations. The ^{18}F decay curve measured with the Betabox (blue dots) accurately matches the known half-life of ^{18}F of 109.8 min (red line).

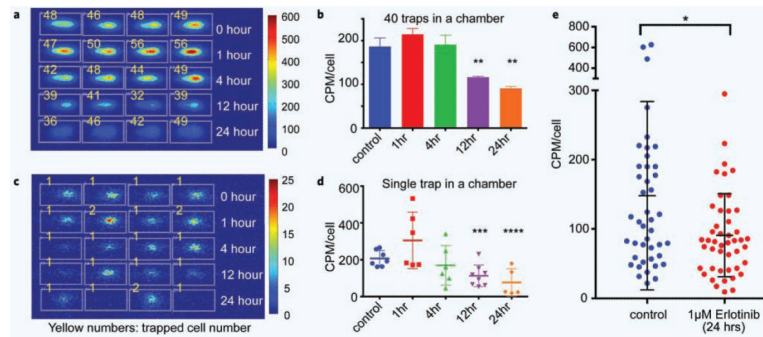


Figure 3. Betabox measurements of GBM39 cells with erlotinib treatment. **(a)** Image of the ¹⁸F activity from 30–60 GBM39 cells/chamber treated with erlotinib for various treatment times (0, 1, 4, 12, and 24 hours). Rectangular regions of interest (ROI) are shown as white boxes from which the total signal activities from the corresponding chambers were collected. For each ROI, the number of trapped cells is given in yellow font. **(b)** The average measured ¹⁸F activity per cell from **(a)**. **(c)** Image of the ¹⁸F activity from GBM39 single cells treated with erlotinib for various treatment times (0, 1, 4, 12, and 24 hours). **(d)** Measured ¹⁸F activity per cell from **(c)**. **(e)** ¹⁸F activity from GBM39 single cells with/without erlotinib treatment measured with five sets of microfluidic chips per condition. Statistical analysis was performed using the two-tailed *t*-test. * $p < 0.05$; ** $p < 0.005$; *** $p < 0.0005$; **** $p < 0.0001$ compared with the control group. CPM: count per minute.

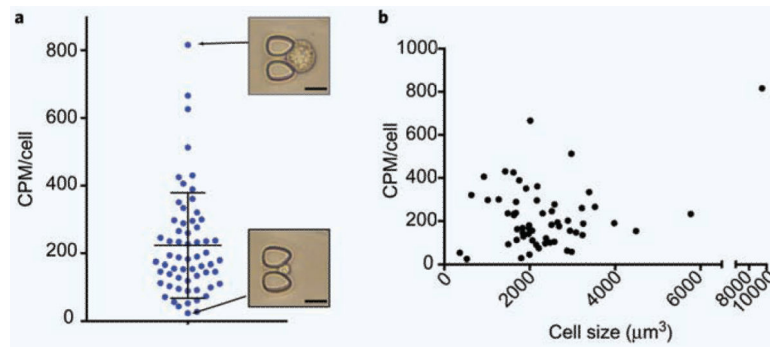


Figure 4. Cell size vs. glycolysis level of GBM39 cells. **(a)** Glycolysis as assayed with ^{18}F -FDG of single GBM39 cells. Representative images of actual cells in two extreme cases are shown as well. **(b)** Scatter plot of glycolysis vs. cell size shows a weak correlation between the two parameters for 58 single cells. Scale bars: 20 μm .